ATMOSPHERIC SCIENCE LETTERS
Atmos. Sci. Let. **14**: 146–152 (2013)
Published online 17 May 2013 in Wiley Online Library
(wileyonlinelibrary.com) **DOI:** 10.1002/asl2.431

RMetS
Royal Meteorological Society

Multiple bands near fronts in VHF wind-profiling radar and radiosonde data

John Lawson,[1,2] David M. Schultz,[3,4,5]* Geraint Vaughan[3,6] and Daniel J. Kirshbaum[1,7]

[1]*Department of Meteorology, University of Reading, UK*
[2]*Department of Atmospheric Sciences, University of Utah, Salt Lake City, UT, USA*
[3]*Centre for Atmospheric Science, School of Earth, Atmospheric and Environmental Sciences, University of Manchester, UK*
[4]*Division of Atmospheric Science, Department of Physics, University of Helsinki, Finland*
[5]*Finnish Meteorological Institute, Helsinki, Finland*
[6]*National Centre for Atmospheric Science, University of Manchester, UK*
[7]*Department of Atmospheric and Oceanic Sciences, McGill University, Montreal, QC, Canada*

*Correspondence to:
D. M. Schultz, Centre for Atmospheric Science, School of Earth, Atmospheric and Environmental Sciences, University of Manchester, Simon Building, Oxford Road, Manchester M13 9PL, UK.
E-mail: David.Schultz@manchester.ac.uk

Received: 21 December 2012
Revised: 25 March 2013
Accepted: 8 April 2013

Abstract

Fronts passing over the Mesosphere–Stratosphere–Troposphere radar near Aberystwyth, Wales, UK, possessed multiple bands in returned power and vertical shear of the horizontal wind. Warm fronts tended to have more bands than cold fronts. Of 82 bands in power with an associated band in the radiosonde data, 45% were associated with a decrease in specific humidity and an increase in stability (drying stable bands) and 21% were associated with an increase in humidity and a decrease in stability (moistening unstable bands). The radar detects airstream boundaries near fronts, some of which are not part of the front.

Keywords: **banding; cold fronts; MST radar; warm fronts; wind shear**

1. Introduction

Fronts are sloping boundaries between warm and cold air masses in the troposphere. Although the classic depiction of a front in conceptual models is a single region of sloping wind shear (Bjerknes, 1935), sometimes observed fronts have multiple regions of wind shear (Röttger, 1979; Browning *et al*., 1998; Schultz and Steenburgh, 1999; Browning, 2005; Schultz, 2005, 2008; Antonescu *et al*., 2013).

To explore the prevalence of such multiple regions of wind shear, Lawson *et al*. (2011) constructed a two-year climatology of 296 frontal passages using data from the vertically pointing, wind-profiling, Mesosphere–Stratosphere–Troposphere (MST) radar at Capel Dewi, near Aberystwyth, Wales. They identified two types of bands. Sloping maxima of vertical shear of the horizontal wind in MST data (hereafter *shear bands*) associated with frontal zones are related to horizontal temperature gradients as required by thermal wind balance. By comparison, bands of maximum radar return signal power (hereafter *power bands*) can be caused by turbulence, vertical gradients in specific humidity q, and vertical gradients in potential temperature θ. These three causes of power bands, along with shear bands, can coincide with frontal zones or coincide with other airstream boundaries (Carlson, 1980; Cohen and Kreitzberg, 1997; Cohen and Schultz, 2005).

In this 2-year period, Lawson *et al*. (2011) found that 74% of the warm fronts were associated with multiple sloping bands of vertical shear of the horizontal wind or radar return signal power in the MST data (a measure of humidity and stability gradients, as shown in Section 2), whereas only 17% of cold fronts were associated with such multiple bands. Why warm fronts were much more likely to possess multiple bands than cold fronts is not known. Even the causes of these bands in the MST radar data have not been explored previously.

This article has two purposes: to determine the characteristics of bands associated with fronts by comparing MST radar data to radiosonde data and to understand why warm fronts tend to be associated with more bands than cold fronts. To make the study manageable, we examine a 1-year catalogue of frontal passages over the MST radar, classifying the various bands that occur in data from the MST radar and from a nearby radiosonde site. An overview of the MST radar is given in Section 2. Section 3 describes the method to identify bands in the MST radar data and any corresponding features in the sounding data. Results

for power and shear bands are presented in Sections 4 and 5, respectively. Section 6 concludes this article.

2. The MST radar

The MST radar (Vaughan, 2002; http://mst.nerc.ac.uk) at Capel Dewi, Aberystwyth, Wales, UK (52.4°N, 4.0°W, 50 m above mean sea level), profiles the atmosphere at altitudes higher than 2 km above ground level every 2 min with gate spacing 150 m. Better coverage and signal-to-noise ratio are obtained with longer radar pulses, so the data presented in this article were all collected with 300-m vertical resolution. Clear-air scattering of 46.5-MHz Very High Frequency (VHF) radiation can result from active turbulence, where return signal power comes from fluctuations in refractive index on the scale of about 3 m, or half the radar wavelength. More commonly, radar echoes come from Fresnel scattering (Gage *et al*., 1981), caused by pancake-like structures in refractive index. Both humidity and temperature affect the index of refraction, so gradients in humidity and temperature will affect the return signal power, leading to maxima in the radar profile (bands, when viewed in a time–height vertical cross-section).

Return signal power depends upon M, the gradient of the potential refractive index of air with height z (hereafter *potential refractivity*). Specifically, the return signal power measured in dB is proportional to $\log(M^2/z^2)$ (Gage and Balsley, 1980), where M is computed using Equation (2) in Vaughan and Worthington (2000):

$$M = -77.6 \times 10^{-6} \frac{p}{T} \left(\frac{\partial ln\theta}{\partial z} + \frac{15500q}{T} \frac{\partial ln\theta}{\partial z} - \frac{7750}{T} \frac{\partial q}{\partial z} \right), \quad (1)$$

where p is pressure (hPa), T is temperature (K), θ is potential temperature (K), and q is specific humidity (kg kg^{-1}).

The opposite signs between the stability terms and the moisture-gradient term on the right-hand side of Equation (1) can be explained physically as follows. The refractive index of air increases roughly linearly with density. Because density decreases most rapidly when potential temperature increases rapidly, a positive $\partial\, ln\theta/\partial z$ is associated with a refractive index decreasing with height. In contrast, water vapour (being a polar molecule) increases the refractive index. Consequently, a positive $\partial\, q/\partial z$ is associated with a refractive index increasing with height. For the upper troposphere, the MST data are particularly well suited to identify the tropopause, where high power is returned from the high static stability there. In the lower troposphere, however, specific humidity gradients dominate the power (May *et al*., 1991; Vaughan and Worthington, 2000). A departure from the general dependence of power on $\log(M^2/z^2)$ occurs in precipitation, especially stratiform precipitation which causes a greater suppression of the signal than convective precipitation (Vaughan and Worthington, 2000; McDonald *et al*., 2006).

The radar also measures the three-dimensional wind speed and direction, allowing for calculation of the magnitude of the vertical shear of the horizontal wind ($\mathbf{V} = u\hat{\imath} + v\hat{\jmath}$):

$$\left|\frac{d\mathbf{V}}{dz}\right| = \sqrt{\frac{du}{dz}^2 + \frac{dv}{dz}^2} \quad (2)$$

3. Method

We use the dataset of frontal passages developed in Lawson *et al*. (2011). These data were compiled by identifying all cold, warm, and occluded fronts that passed Capel Dewi in 2004 and 2005 on the Deutscher Wetterdienst (DWD) surface analyses (Lawson *et al*., 2011). Two-hundred and ninety-six fronts were identified during this 2-year period. To reduce the large number of cases into a manageable size for manual analysis, however, we consider only the 138 fronts during 2004. These fronts consisted of 68 cold fronts, 41 warm fronts, and 29 occluded fronts.

To determine the physical characteristics of bands associated with frontal passages from the MST data, we compare the MST radar data to upper-air data from the nearest sounding station, Aberporth, which is 51 km southwest of Capel Dewi. The upper-air data were collected every 2 s as the balloon rose and were archived at the British Atmospheric Data Centre (BADC). Unfortunately, because Aberporth is not an operational site with twice-daily soundings, the Aberporth data were not regularly available each day throughout the year, and most of the available Aberporth soundings in 2004 were released at 0600 UTC.

Sixty Aberporth soundings intersected at least one of the 138 fronts in the MST radar data between 2 km above ground level and the tropopause. Ten of the 60 profiles were not considered further because incomplete MST or sounding data prevented a complete analysis, reducing the dataset to 50 profiles. Within these 50 profiles, three profiles intersected two different fronts within one ascent. These three profiles all intersected what appeared to be a surface-based cold front underneath a band oriented in the opposite direction that looked like a tropopause fold. Bands associated with these three tropopause folds descended with time sufficiently close to an analysed warm front and were hence deemed part of the warm-frontal system. As this study focusses on multiple bands associated with one front, these three profiles of six fronts were not studied further. Moreover, a frontal passage was captured by more than one profile on 11 occasions, but these cases were retained in this dataset. Therefore, the dataset comprised 47 profiles of 33 unique fronts. Within the 47 profiles, 125 MST bands were identified following the methodology in Lawson *et al*. (2011): 56 associated with power only,

27 associated with shear only, and 42 associated with both. The band associated with the quasi-horizontal tropopause was not considered in this study.

To make a direct comparison between the 98 MST power bands and sounding data, the profile of radar return signal power was estimated by calculating $\log(M^2/z^2)$ as a function of height from the sounding data using Equation (1). The altitude of the $\log(M^2/z^2)$ maximum nearest to each MST power band, within a range of ± 1 km, was recorded to the nearest 0.1 km. Where there was no obvious corresponding maximum in $\log(M^2/z^2)$, or where it was unclear which maximum corresponded to the band, that band was not included in subsequent statistics. Sixteen bands were excluded due to these criteria, leaving 82 power bands in the radar data having a corresponding $\log(M^2/z^2)$ maximum in the sounding data.

A similar method was employed to relate shear derived from the radar data and shear measured from the sounding data. The magnitude of the shear $\left|\frac{d\mathbf{V}}{dz}\right|$ and its derivative $\frac{d}{dz}\left|\frac{d\mathbf{V}}{dz}\right|$ from the radiosonde data were calculated. A maximum in shear in the radiosonde data corresponded to a maximum in shear in the MST data (i.e. a shear band) if (1) the maximum in $\left|\frac{d\mathbf{V}}{dz}\right|$ from the radiosonde data occurred within 1 km of either side of the MST band, (2) the maximum in $\left|\frac{d\mathbf{V}}{dz}\right|$ was greater than 15 m s^{-1} km^{-1}, and (c) $\frac{d}{dz}\left|\frac{d\mathbf{V}}{dz}\right|$ was greater than 20 m s^{-1} km^{-2} below the band and less than -20 m s^{-1} km^{-2} above the band. These three criteria were applied (a) to allow for the frontal slope, the distance between the MST radar and the radiosonde site, and drift of the radiosonde with the wind, (b) to ensure that the maxima that are picked are of sufficient intensity, and (c) to account for the typical intensity of MST shear bands, which are about 10 m s^{-1} km^{-1} greater than the environmental shear (around 5 m s^{-1} km^{-1}). The threshold value of shear magnitude gradient is derived by dividing the typical maximum of an MST shear band (15 m s^{-1} km^{-1}) by 0.75 km, or half the depth of a typical band, to yield 20 m s^{-1} km^{-2}. Of the 69 bands associated with wind shear, 45 (65%) had corresponding shear maxima in sounding data. Radiosonde-derived shear was also compared to MST power bands within ± 1 km.

As an illustration of these methods, consider the case of 31 May to 3 June 2004. This event was associated with a surface warm-frontal passage over the UK on 3 June 2004 (Figure 1). The MST radar data show two dominant bands of high power descending from the wind maximum in the middle and upper troposphere beginning around 1800 UTC 31 May (Figure 2). By 0700 UTC 1 June, a third dominant power band started to descend. By the time of the Aberporth sounding at 0600 UTC 2 June (Figure 3), the lowest of the three bands had descended below the lowest MST radar gate near 2 km, leaving two bands at 3 and 4 km (Figure 2). Calculating the power from Equation (1) and the Aberporth sounding data reveals maxima in power at 3.1 and 4.4 km (red line in Figure 4), corresponding to similar bands in the MST data (black line in Figure 4). If the specific humidity is set to zero in Equation (1), then the effect of the static stability alone can be seen (blue line in Figure 4). There is a closer correspondence between Equation (1) and Equation (1) with the dry term only (by setting $q = 0$) above about 4.5 km where the gradients of specific humidity are smaller. In contrast, in the lower troposphere where moisture gradients are larger (cf. red and

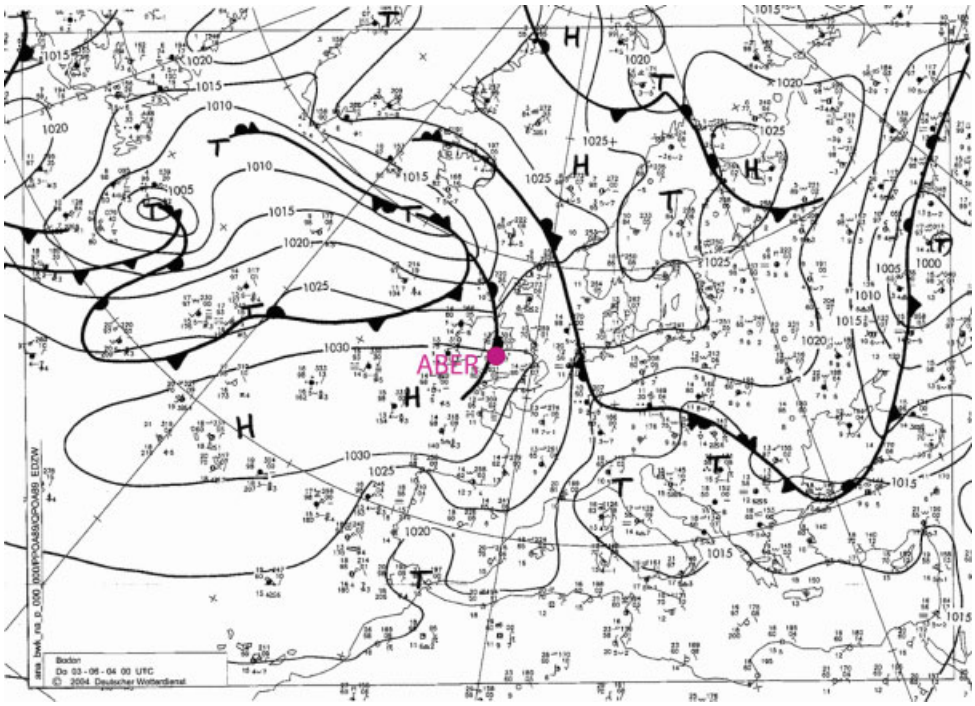

Figure 1. Surface analysis from Deutsche Wetterdienst at 0000 UTC 3 June 2004. Pink circle labeled 'ABER' indicate location of MST radar in Aberystwyth and radiosounding location in Aberporth. Image courtesy of wetter3.de.

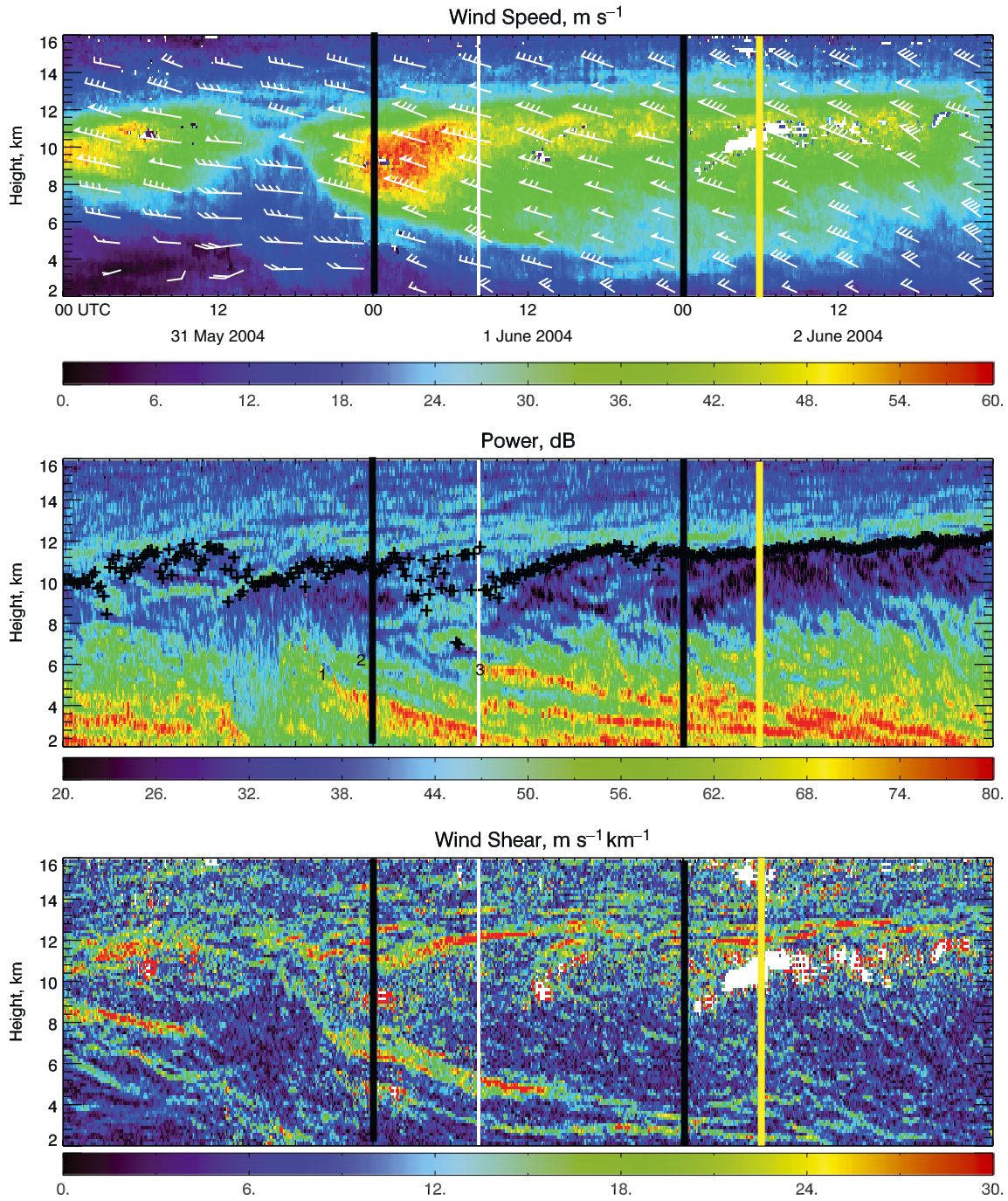

Figure 2. Data from the MST radar from 0000 UTC 31 May 2004 to 2359 UTC 2 June 2004: (top) wind speed (m s^{-1}) and wind direction (pennant, full barb, and half-barb denote 25, 5, and 2.5 m s^{-1}, respectively); (middle) signal power (dB) and tropopause (black crosses); and (bottom) magnitude of the vertical shear of the horizontal wind (m s^{-1} km^{-1}). The white line at 0700 UTC 1 June refers to the third dominant power band starting to descend, and the yellow line at 0600 UTC 2 June represents the sounding release from Aberporth. Black lines at 0000 UTC represent midnight. Bands are labelled 1, 2, and 3.

blue lines in Figure 4), the importance of the moisture terms is much greater, confirming previous results (May *et al*., 1991; Vaughan and Worthington, 2000). Although the wind shear has more structure (Figures 2 and 5), bands of maximum shear from the MST around 2.5, 3.6, and 4.5 km are evident at the time of the sounding, with a close correspondence between the MST shear and radiosonde shear. This warm front displays multiple power and shear bands, similar to many of the other warm fronts in this dataset. Therefore, this case shows the complexity of the wind field near fronts (Röttger, 1979; Schultz and Steenburgh, 1999; Schultz, 2005, 2008; Antonescu *et al*., 2013).

4. Bands in power

Of the 98 power bands from the MST radar data, 82 (84%) possessed a corresponding maximum in $\log(M^2/z^2)$ from radiosonde data. To understand the

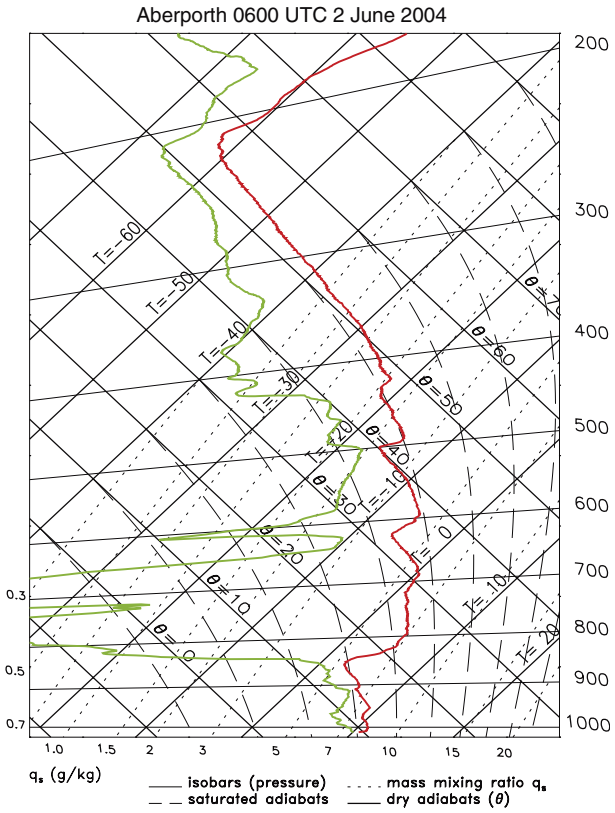

Figure 3. Aberporth sounding at 0600 UTC 2 June 2004.

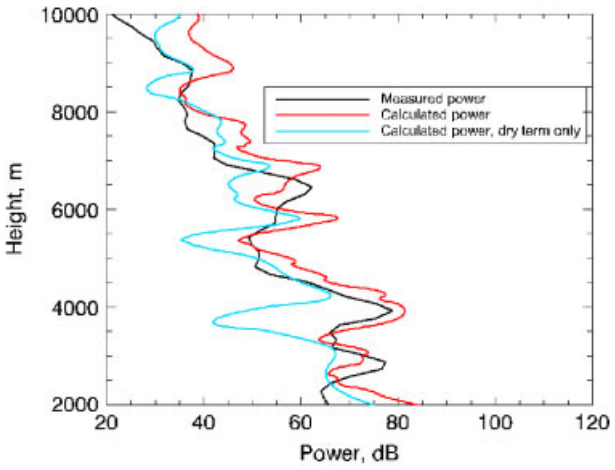

Figure 4. Measured power from the MST radar data (black line) versus calculated power from the Aberporth sounding at 0600 UTC 2 June 2004 (red line) (dB). The blue line represents the calculated power from Equation (1) with the dry term only (by setting $q = 0$).

physical characteristics of these 82 power bands, profiles of dq/dz and $d\theta/dz$ for each of the 82 bands were determined and each band in each of the profiles was classified as a maximum, minimum, or neither. Of the nine possible combinations of dq/dz and $d\theta/dz$, three groups were predominant. The most commonly occurring group (37 group-1 bands, or 45% of the 82 bands) was characterized by a minimum of dq/dz and a maximum of $d\theta/dz$ (drying stable band). Figure 3 provides some examples of group-1 bands. Of the 47

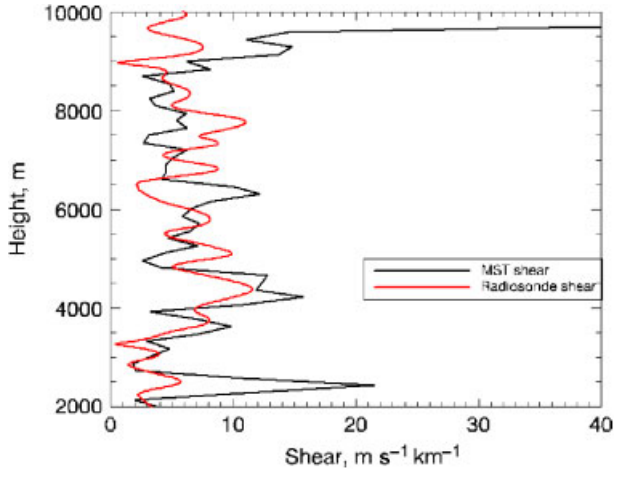

Figure 5. Calculated magnitude of the vertical shear of the horizontal wind from the MST radar data (black line) versus that from the Aberporth sounding (red line) at 0600 UTC 2 June 2004 (m s^{-1} km^{-1}).

frontal profiles, 25 have at least one group-1 band. The second most commonly occurring group (17 group-2 bands, or 21%) was characterized by a maximum in dq/dz and a minimum in $d\theta/dz$ (moistening, less stable band). The third most commonly occurring group (12 group-3 bands, or 15%) was characterized by a maximum in dq/dz and a maximum in $d\theta/dz$ (moistening stable band). The six remaining groups containing 16 bands (20%) were combined into a fourth group called 'Others', which is not discussed further in this article.

A simple explanation underlies the dominance of these three groups. In the expression for M (Equation (1)), the two static stability terms are of opposite sign to the term with the vertical derivative of specific humidity. As discussed previously, these opposite terms have physical meaning: strong static stability is associated with refractive index decreasing with height ($M < 0$), whereas specific humidity increasing with height is associated with a refractive index increasing with height ($M > 0$). Thus, $|M|$ is large when the static stability is large and the specific humidity decreases with height (group-1 bands) and when the static stability is small and the specific humidity increases with height (group-2 bands). These occurrences would be when the stability and moisture terms both contribute to large $|M|$. The third most common group of bands (group-3 bands, when the static stability is large and the specific humidity increases with height) occurs because the specific humidity term dominates the static stability term (May *et al*., 1991). Other combinations of stability and moisture gradients are not favourable for large values of $|M|$, which explains why they are not common.

As in Lawson *et al*. (2011), each of the four band groups was then categorized by the type of associated front: cold front, warm front, cold-frontal segment of an occluded front, and warm-frontal segment of an occluded front (Table I). Most of the 82 bands occurred with warm fronts (43 or 52%)

Table I. Classification of different types of bands by the type of associated front. See text for description of the different band types.

Type of front	Group 1 band drying stable	Group 2 band moistening unstable	Group 3 band moistening stable	Other bands	Total
Warm	23	11	4	5	43
Cold	4	0	2	2	8
Occluded: warm-frontal segment	8	3	6	9	26
Occluded: cold-frontal segment	2	3	0	0	5
Total	37	17	12	16	82

and warm-frontal segments of occluded fronts (26 or 32%). Of the 43 bands associated with warm fronts and the 26 bands associated with warm-frontal segments of occluded fronts, almost half (31 or 45%) were stable and dry (group 1). The small sample size of many of the groups in Table I precludes more detailed analysis on those groups.

To better understand the synoptic environments in which multiple bands occur, we considered the 33 profiles in which multiple power bands occurred in MST data and only one front was intersected. Of these 33 profiles, 25 (76%) were associated with multiple $\log(M^2/z^2)$ maxima. Of these 25 profiles, 13 were warm fronts, 9 were warm-frontal segments of occluded fronts, 2 were cold fronts, and 1 was a cold-frontal segment of an occluded front. The large number of warm fronts and warm-frontal segments of occluded fronts that correspond with multiple power bands resembles the similar warm-frontal dominance of multiple bands in both power and shear in Lawson *et al*. (2011, their Figure 4). Given the strong dependence of power on static stability, that warm fronts are more likely to be associated with bands makes sense because cold-frontal zones tend to be less statically stable (Schultz, 2008; Schultz and Roebber, 2008; Schultz and Vaughan, 2011, p. 454).

5. Bands in shear

By comparison, 20 profiles intersected only one front and were associated with multiple shear bands in the MST data. Of these 20 profiles, 12 (60%) were associated with multiple shear bands in radiosonde data. Of these 12 profiles, 5 were warm fronts, 5 were warm-frontal segments of occluded fronts, 1 was a cold front, and 1 was a cold-frontal segment of an occluded front.

Data from the 69 MST shear bands were compared to the radiosonde-derived shear. Of the 69 bands, 45 (65%) occurred with a shear maximum in radiosonde data. MST power-only bands were associated with shear maxima in the profile data in 22 of 57 (39%) bands. Thus, 39% of bands in wind shear were also associated with a change in stability or moisture (through the power term), suggesting that these may be airstream boundaries and fronts. Of the 69 MST shear bands, 31 were associated with warm fronts, 23 with warm-frontal segments of occluded fronts, 11 with cold fronts, and 4 with cold-frontal segments of occluded fronts. Thus, multiple bands – whether identified in the MST data by power (stability and humidity gradients) or shear – were more common in association with warm fronts and warm-frontal segments of occluded fronts than cold fronts and cold-frontal segments of occluded fronts (Lawson *et al*., 2011).

6. Conclusion

Lawson *et al*. (2011) demonstrated that many fronts detected with a VHF wind-profiling radar were associated with multiple bands in power and shear and that warm fronts were more likely to be associated with multiple bands than cold fronts. The purpose of this article is to determine the characteristics of those bands by comparing MST radar data to radiosonde data and to understand the reasons for the larger number of bands associated with warm fronts. In 2004, 33 fronts that passed over the Mesosphere–Stratosphere–Troposphere radar near Aberystwyth, Wales, UK, served as the principal dataset for this study. Of 82 bands in power with an associated radiosonde profile, 45% were stable bands with a decrease in specific humidity (drying stable band) and 21% were unstable bands associated with an increase in specific humidity (moistening unstable band). The third most common group encompassed 15% of the bands, which were stable and associated with an increase in specific humidity (moistening stable band).

Warm fronts are commonly associated with power bands because of their strong stability, which tends to increase the returned power from the radar. Warm fronts are associated with more shear bands, too. Previously published case studies show that many warm fronts, in particular, resemble tropopause folds, and these warm fronts occur in air masses with multiple airstream boundaries (Antonescu *et al*., 2013). The result is that determining the frontal position in cross-sections can be difficult. Because cold-frontal zones are less statically stable, they are less clearly observed with the MST radar. Finally, the complexity of some of the banding structures in these cases (i.e. profiles with three or more bands) suggests that fronts may often be more complex than the simple pictures painted by conceptual models.

Acknowledgements

We thank David Hooper, project scientist for the MST radar, for providing the radar data. Radar imagery was taken from the quick-look plots produced by BADC. BADC also supplied the 2-s radiosonde data. The Aberporth sounding data was obtained from the University of Wyoming website (http://weather.uwyo.edu/upperair/sounding.html). We thank Robert Cohen and two anonymous reviewers for their comments that improved this article. This research is a continuation of Lawson's 2010 NERC-funded Research Experience Placement. Partial funding for Lawson and Schultz came from grant 126853 from the Academy of Finland. Partial funding for Schultz also came from Vaisala Oyj.

References

Antonescu B, Vaughan G, Schultz DM. 2013. A five-year radar-based climatology of tropopause folds and deep convection over Wales, United Kingdom. *Monthly Weather Review* **140**: DOI: 10.1175/MWR-D-12-00246.1.

Bjerknes J. 1935. Investigations of selected European cyclones by means of serial ascents. *Geofysiske Publikasjoner* **11** (4): 3–18.

Browning KA. 2005. Observational synthesis of mesoscale structures within an explosively developing cyclone. *Quarterly Journal of the Royal Meteorological Society* **131**: 603–623.

Browning KA, Jerrett D, Nash J, Oakley T, Roberts NM. 1998. Cold frontal structure derived from radar wind profilers. *Meteorological Applications* **5**: 67–74.

Carlson TN. 1980. Airflow through midlatitude cyclones and the comma cloud pattern. *Monthly Weather Review* **108**: 1498–1509.

Cohen RA, Kreitzberg CW. 1997. Airstream boundaries in numerical weather simulations. *Monthly Weather Review* **125**: 168–183.

Cohen RA, Schultz DM. 2005. Contraction rate and its relationship to frontogenesis, the Lyapunov exponent, fluid trapping, and airstream boundaries. *Monthly Weather Review* **133**: 1353–1369.

Gage KS, Balsley BB. 1980. On the scattering and reflection mechanisms contributing to clear air radar echoes from the troposphere, stratosphere, and mesophere. *Radio Science* **15**: 243–257.

Gage KS, Balsley BB, Green JL. 1981. Fresnel scattering model for the specular echoes observed by VHF radar. *Radio Science* **16**: 1447–1453.

Lawson J, Vaughan G, Schultz DM. 2011. Classifying fronts in data from a VHF wind-profiling radar. *Atmospheric Science Letters* **12**: 375–380.

May PT, Yamamoto M, Fukao S, Sato T, Kato S, Tsuda T. 1991. Wind and reflectivity fields around fronts observed with a VHF radar. *Radio Science* **26**: 1245–1249.

McDonald AJ, Monahan KP, Cooper DA, Gaffard C. 2006. VHF signal power suppression in stratiform and convective precipitation. *Annales Geophysicae* **24**: 23–35.

Röttger J. 1979. VHF radar observations of a frontal passage. *Journal of Applied Meteorology* **18**: 85–91.

Schultz DM. 2005. A review of cold fronts with prefrontal troughs and wind shifts. *Monthly Weather Review* **133**: 2449–2472.

Schultz DM. 2008. Perspectives on Fred Sanders' research on cold fronts. *Synoptic-Dynamic Meteorology and Weather Analysis and Forecasting: A Tribute to Fred Sanders, Meteorological Monographs*, No. 55. American Meteorological Society; 109–126. Boston, Massachusetts, USA.

Schultz DM, Roebber PJ. 2008. The fiftieth anniversary of Sanders (1955): a mesoscale-model simulation of the cold front of 17–18 April 1953. *Synoptic-Dynamic Meteorology and Weather Analysis and Forecasting: A Tribute to Fred Sanders, Meteorological Monographs*, No. 55. American Meteorological Society; 126–143. Boston, Massachusetts, USA.

Schultz DM, Steenburgh WJ. 1999. The formation of a forward-tilting cold front with multiple cloud bands during Superstorm 1993. *Monthly Weather Review* **127**: 1108–1124.

Schultz DM, Vaughan G. 2011. Occluded fronts and the occlusion process: a fresh look at conventional wisdom. *Bulletin of the American Meteorological Society* **92**: 443–466, ES19–ES20.

Vaughan G. 2002. The UK MST radar. *Weather* **57**: 69–73.

Vaughan G, Worthington RM. 2000. Effects of humidity and precipitation on VHF radar vertical beam echoes. *Radio Science* **35**: 1389–1398.